Empirical State-Space Modeling for Epileptic Brain Dynamics

Weng Ruihong1,2, Na Xiao1,2, Zezhou Zhang3, Paddy K. L. Chan1,2*
*Corresponding Author: pklc@hku.hk

1. Department of Mechanical Engineering, The University of Hong Kong, Hong Kong.
2. Advanced Biomedical Instrumentation Centre, Hong Kong.
3. Department of Mechanical and Aerospace Engineering, Rutgers, the State University of New Jersey, USA

Introduction

While conventional EEG analysis relies on descriptive metrics like amplitude, frequency, or connectivity, Dynamic Systems Theory (DST) offers a framework for modeling and analyzing the mechanisms governing neural processes. However, a long-standing gap remains between bottom-up and top-down modeling approaches: biophysical models struggle to precisely fit real neural signals, whereas data-driven methods lack interpretability.

We bridge this gap with MAVEN (Mamba-based Adaptive Virtual Epileptic Network), a hybrid framework integrating a deep state-space backbone with biophysical constraints. MAVEN performs adaptive system identification, learning governing equations directly from EEG recordings to reconstruct the underlying epileptic manifold. This novel approach supports four key clinical applications:

1. Optimized Neuromodulation: MAVEN achieves accurate, long-horizon forecasting of epileptic signals with or without stimulation. This capability is the essential prerequisite for developing optimized, closed-loop stimulation protocols.
2. Robust SOZ Localization: By analyzing learned system parameters, MAVEN distinguishes Seizure Onset Zones with superior cross-subject generalization compared to raw signal.
3. Dynamic Functional Connectivity: MAVEN's explicit modeling of coupling parameters offers a mechanistic, time-varying measure of effective connectivity, capturing evolving propagation networks beyond static correlation.
4. Precision Biomarkers: MAVEN uncovers a low-dimensional bistable manifold conserved across species. This dynamical signature may relate to ion channel dysfunction and serve as a novel biomarker for precision medicine, targeted drug selection, and personalized neuromodulation.

Methods: Model architecture

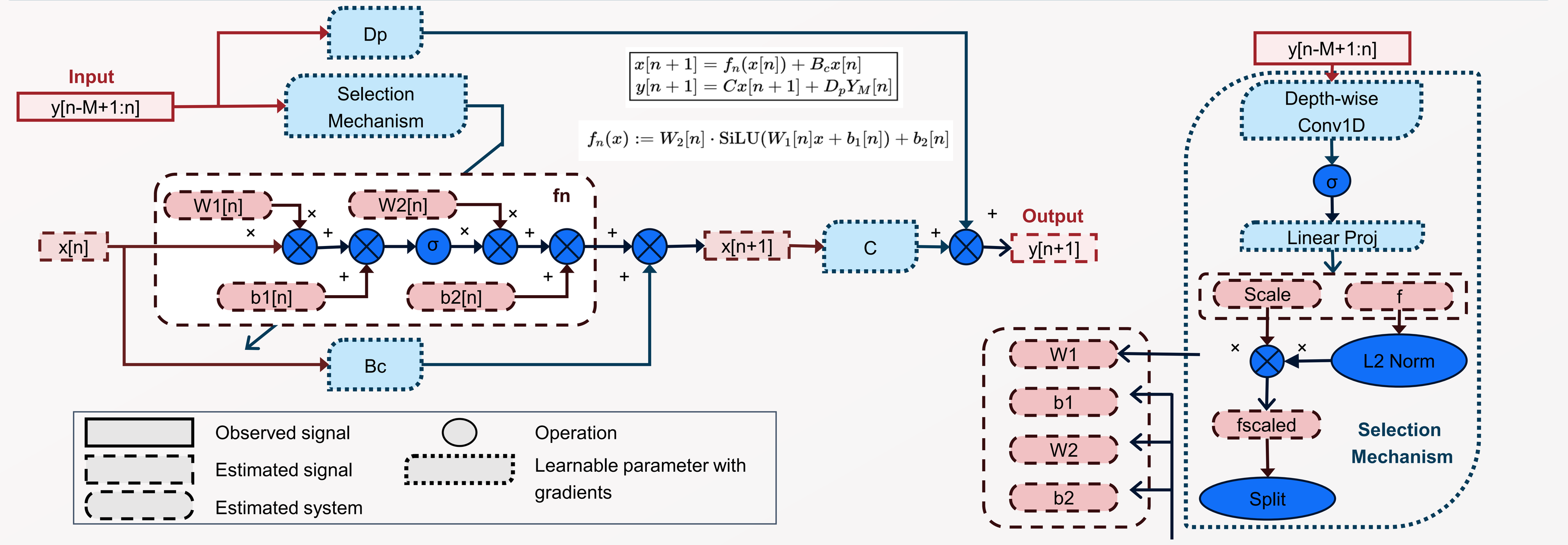

Methods: Experiment setting

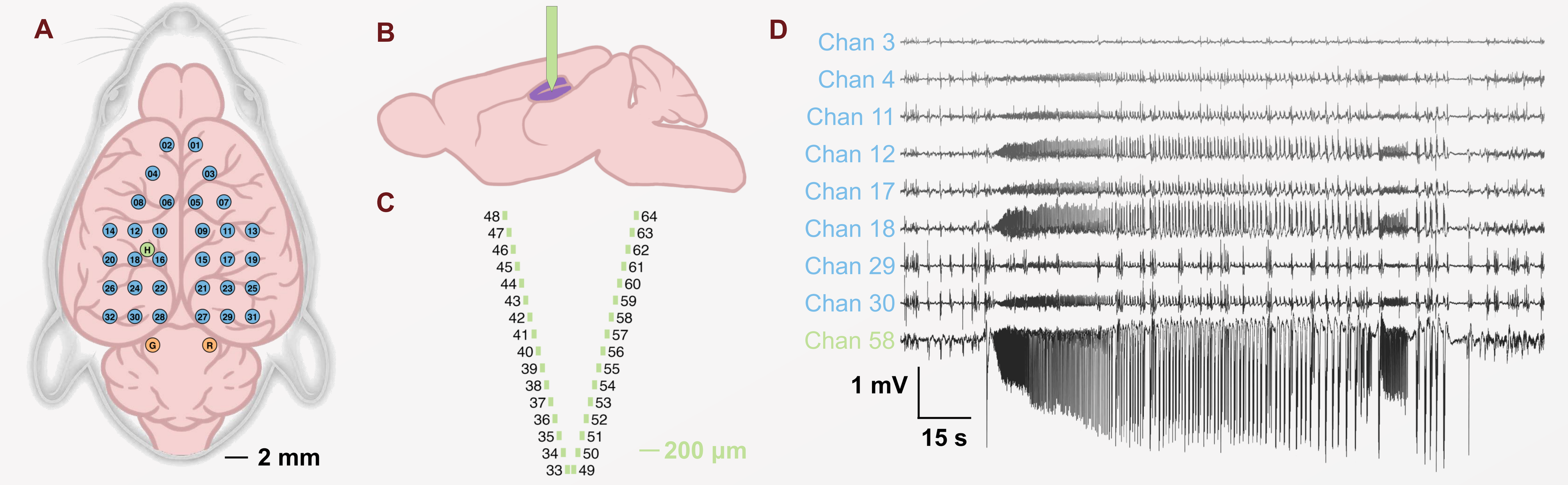

Adult male Sprague-Dawley rats (n=10) were implanted with a 32-channel ECoG array secured via cranial screws for global cortical monitoring and a 32-channel intracortical soft probe at the left hippocampus (n=6) and right hippocampus (n=4) for local field potential recording. Simultaneous cortical and hippocampal signals were acquired using a Blackrock Neural Signal Processor (0.3–150 Hz bandpass, 1000 Hz sampling rate). Acute seizures were induced by microinjection of 4-aminopyridine (4-AP) into the hippocampal CA1 region. To investigate specific neuromodulation, two rats received stereotaxic injections of the viral vector AAV2/9-ChR2(H134R)-mCherry into the target hippocampal region to express channelrhodopsin-2. Following viral transduction, optical fibers were chronically implanted above the injection site. Optogenetic stimulation was delivered using a 473 nm blue laser diode with a power density of 3–15 mW/mm².

Applications: Epileptiform signal forecasting

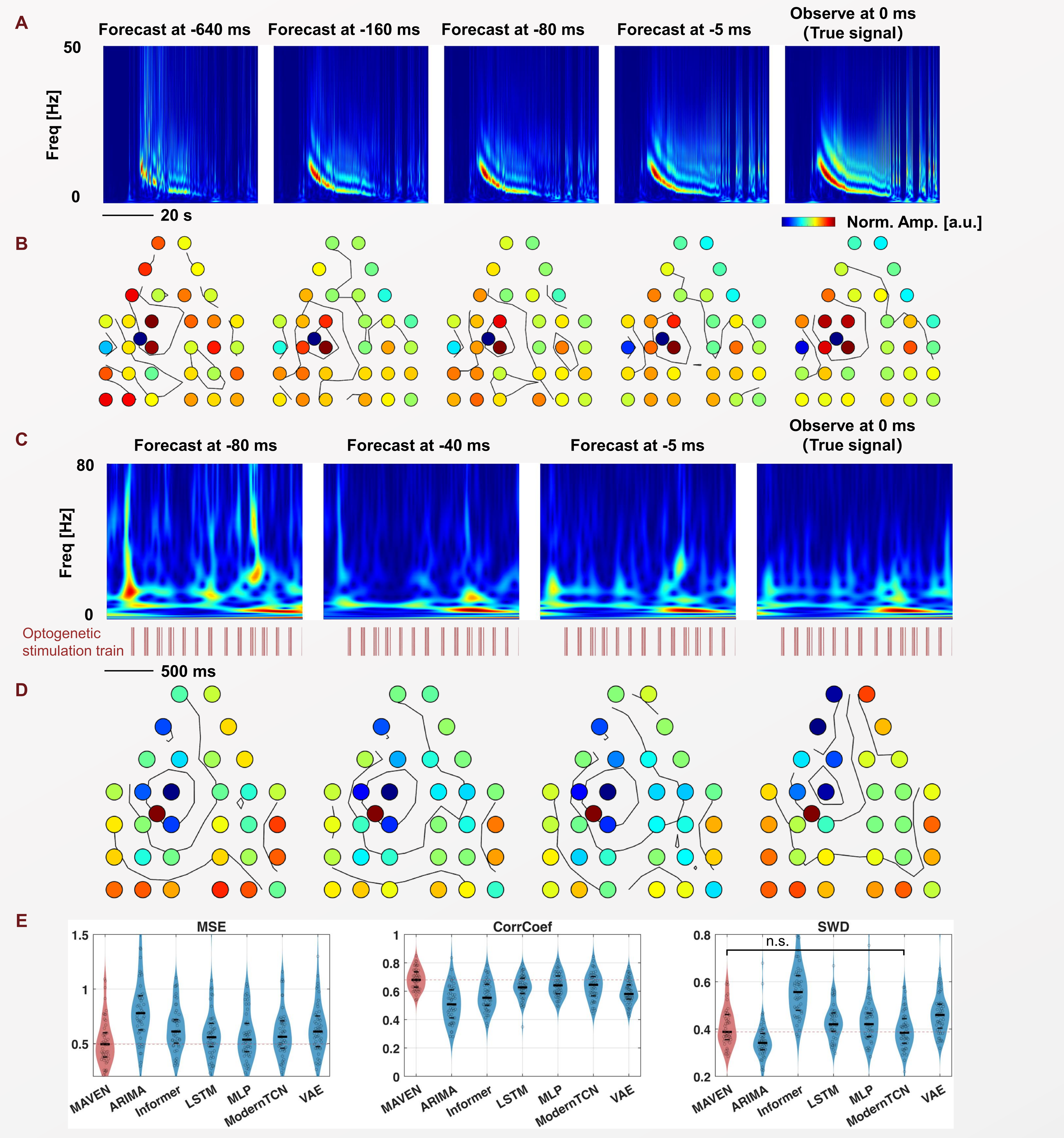

(A) Long-range seizure forecasting. Time-frequency spectrograms showing predicted brain signals at lead times of 640 ms, 160 ms, 80 ms, and 5 ms before the true observed signal at channel 58 (hippocampus). The predicted frequency patterns match the actual observed signal (far right) at long forecast horizons. (B) Spatial energy distribution of seizure activity forecasting. Whole-brain topographic maps corresponding to one timestep at each lead time in (A). The model forecasts the spatial distribution pattern of the seizure across the electrode array, matching the true recording (far right). (C) Forecasting neural response to stimulation. Spectrograms showing real and predicted neural activity during a train of optogenetic stimulation pulses (red vertical lines). (D) Spatial distribution of stimulation response. Topographic maps corresponding to the lead time in (C). (E) Quantitative performance benchmarking. Violin plots comparing the forecasting accuracy of MAVEN (red) against six state-of-the-art baseline models (blue). The metrics shown are Mean Squared Error (MSE, lower is better), Correlation Coefficient (CorrCoef, higher is better), and Sliced Wasserstein Distance (SWD, lower is better). "n.s." indicates non-significant differences at a 5% significant level with a paired t-test.

Accurate forecasting of both intrinsic neural dynamics and their response to stimulation constitutes the essential prerequisite for designing optimized, closed-loop neuromodulation interventions.

Applications: Seizure onset zone localization

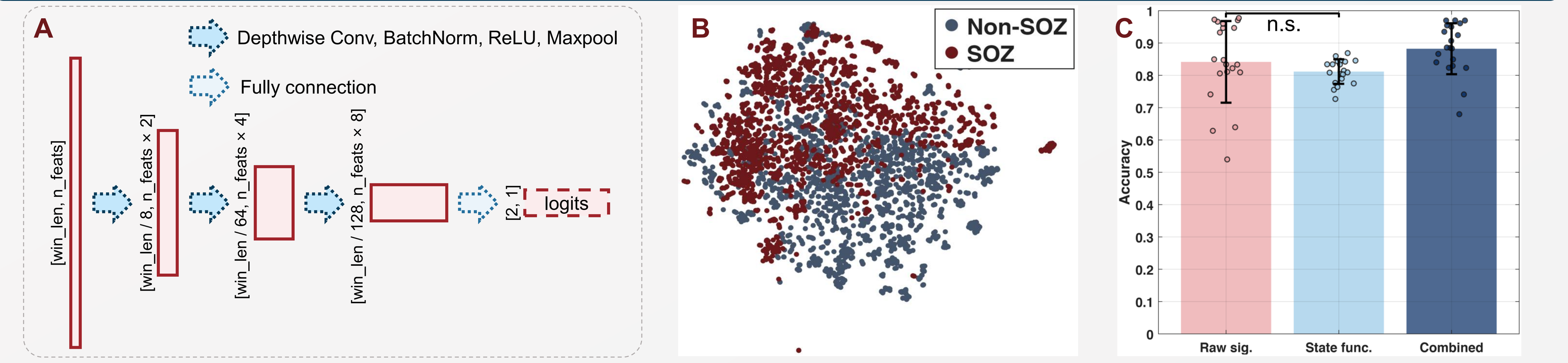

(A) CNN architecture for inter-subject seizure onset zone (SOZ) localization to classify brain regions as either SOZ or Non-SOZ. (B) t-SNE visualization of MAVEN features for SOZ identification. (C) Accuracy of SOZ localization using different feature sets as CNN inputs: raw signal only, state function features, and combined. "n.s." indicates non-significant differences at a 5% significance level with a paired t-test.

Using MAVEN parameters as features significantly enhances the generalization of SOZ localization model across different subjects.

Applications: Functional connectivity estimation

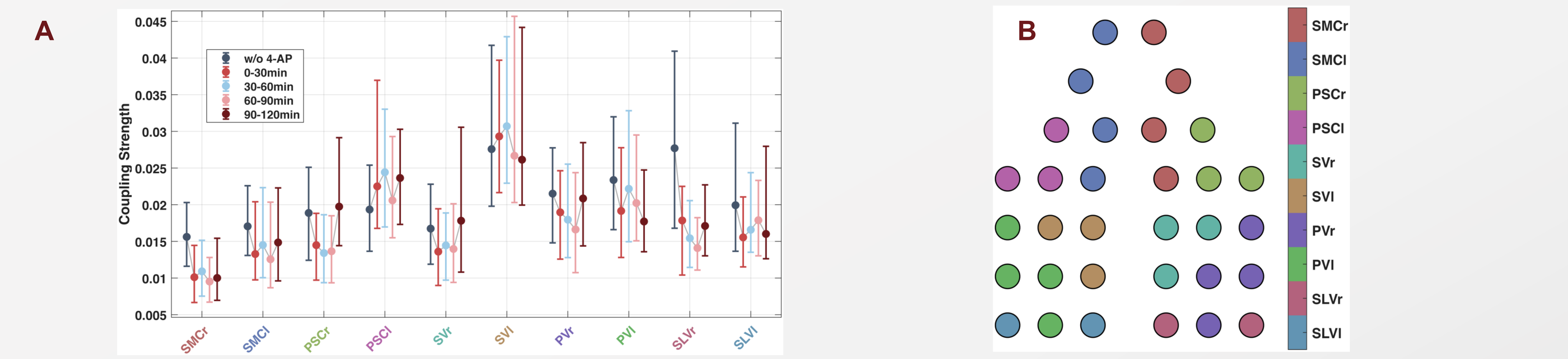

(A) Dynamic coupling strength to the hippocampus. The plot displays the mean coupling strength (with error bars indicating standard deviation) between various targeted cortical regions and the hippocampus across different experimental phases: baseline (w/o 4-AP) and subsequent 30 intervals following 4-AP administration. (B) Illustration of cortical regions.

MAVEN introduces a novel methodology for evaluating functional connectivity by explicitly modeling it within the dynamic system, as an alternative to traditional phase-related (e.g., PLV) or entropy-related (e.g., Mutual Information or Granger causality) measures.

Applications: EEG biomarker targeting

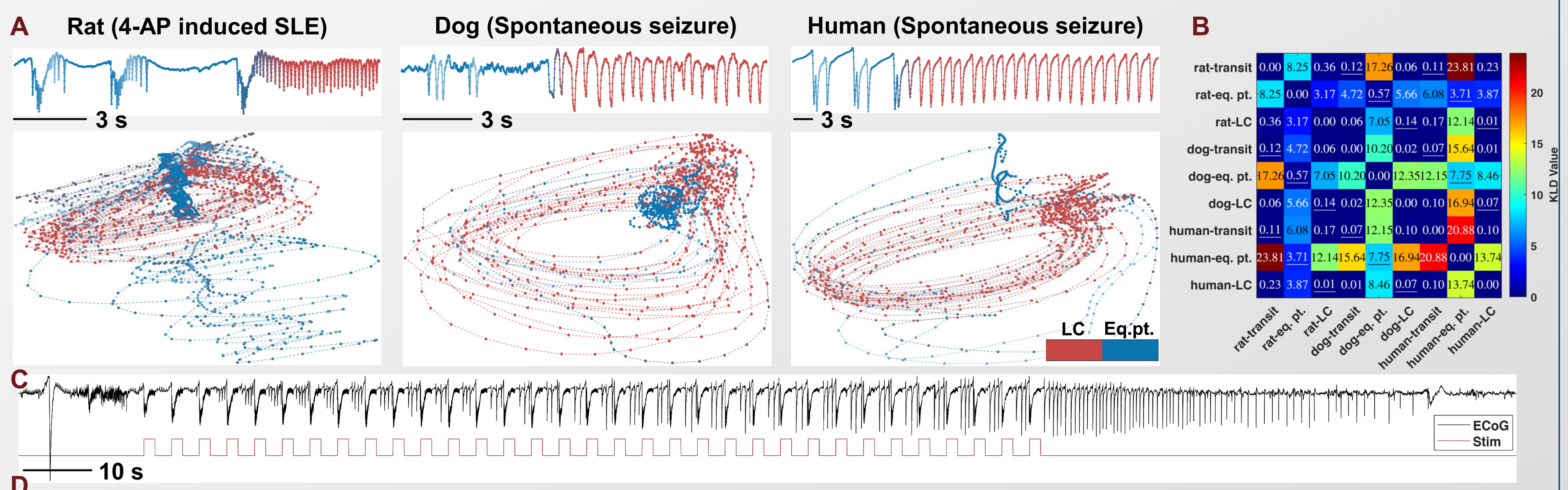

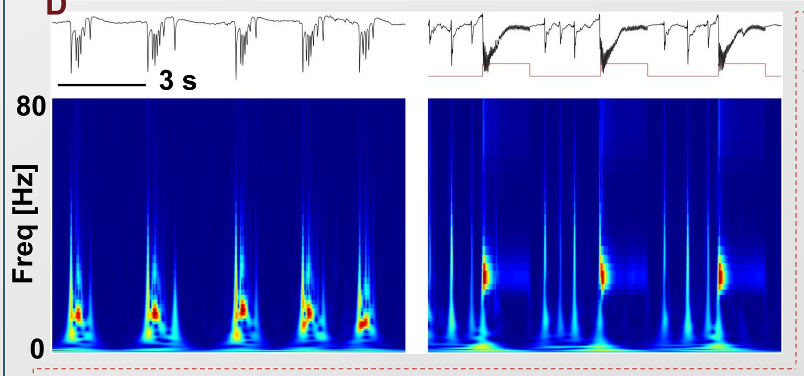

(A) Universal geometry of seizure dynamics. Top: Representative raw signal traces from a rat (induced seizure-like event (SLE)), dog (spontaneous seizure), and human (spontaneous seizure), showing an unstable resting state (blue), epileptiform periodic discharges (red), and their transition. The transition is via a trajectory with rhythmic slow activities and superimposed fast activities (RDA+F). Bottom: The corresponding 3D phase-space manifolds reconstructed by MAVEN. The orbit shows random oscillation around a fixed point (Eq. pt. blue) and a recurrent limit cycle (LC, red). Despite significant differences in the raw waveforms, frequencies, and amplitudes across species, MAVEN reveals a conserved "bistable" geometric structure in all three. (B) Cross-species topological similarity. Kullback-Leibler (KL) divergence (lower values indicate higher similarity) between different dynamic stages (Limit Cycle, Equilibrium Point, Transition) across species. The analysis reveals that specific dynamic stages are structurally more similar across species (e.g., "Human-LC" vs. "Dog-LC") than different states are within the same subject (e.g., "Human-LC" vs. "Human-transit"). (C) Attractor stability under perturbation. The ECoG recording (black) shows the system repeatedly returning to the same periodic discharge rhythm after disruption by optogenetic stimulation (red). This consistent return, combined with a low intrinsic dimension (~4), identifies the LC as a metastable attractor, contrasting with the view that seizures are highly chaotic. (D) Reproduction of biophysical transition orbits. The waveforms (top left) and spectrograms (bottom left) display RDA+F in the rat. Right: using optogenetic stimulation (red trace), we reproduce the RDA+F orbit, aligning with ion dynamics measurements and modeling in the literature, suggesting the featured dynamic pattern may relate to ion channel dysfunction.

This distinct dynamic status in EEG could be a biomarker for precision medicine and personalized neuromodulation.

Reference:

[1] Gu, Albert, and Tri Dao. "Mamba: Linear-time sequence modeling with selective state spaces." *First conference on language modeling*. 2024.
[2] Zhou, Haoyi, et al. "Informer: Beyond efficient transformer for long sequence time-series forecasting." *Proceedings of the AAAI conference on artificial intelligence*. Vol. 35. No. 12. 2021.
[3] Luo, Donghao, and Xue Wang. "Moderntcn: A modern pure convolution structure for general time series analysis." *The twelfth international conference on learning representations*. 2024.
[4] Saggio, Maria Luisa, et al. "A taxonomy of seizure dynamotypes." *Elife* 9 (2020): e55632.
[5] Durstewitz, Daniel, Georgia Koppe, and Max Ingo Thurm. "Reconstructing computational system dynamics from neural data with recurrent neural networks." *Nature Reviews Neuroscience* 24.11 (2023): 693-710.
[6] Bastos, André M., and Jan-Mathijs Schoffelen. "A tutorial review of functional connectivity analysis methods and their interpretational pitfalls." *Frontiers in systems neuroscience* 9 (2016): 175.
[7] Proix, Timothée, et al. "Predicting the spatiotemporal diversity of seizure propagation and termination in human focal epilepsy." Nature communications 9.1 (2018): 1088.
[8] Gnatkovsky, Vadym, et al. "Fast activity at seizure onset is mediated by inhibitory circuits in the entorhinal cortex in vitro." Annals of Neurology: Official Journal of the American Neurological Association and the Child Neurology Society 64.6 (2008): 674-686.
[9] Krishnan, Giri P., and Maxim Bazhenov. "Ionic dynamics mediate spontaneous termination of seizures and postictal depression state." Journal of Neuroscience 31.24 (2011): 8870-8882.
[10] Bonneel, Nicolas, et al. "Sliced and radon wasserstein barycenters of measures." Journal of Mathematical Imaging and Vision 51.1 (2015): 22-45.
[11] Wang, Huifang E., et al. "Delineating epileptogenic networks using brain imaging data and personalized modeling in drug-resistant epilepsy." Science Translational Medicine 15.680 (2023): eabp8982.